RSC Advances

ROYAL SOCIETY OF CHEMISTRY

www.rsc.org/advances

Cite this: DOI: 10.1039/c0xx00000x

www.rsc.org/xxxxxx

ARTICLE TYPE

Efficient electrochemical water oxidation catalysis by nanostructured Mn_2O_3

A. Singh,*[a] D. Roy Chowdhury,[b] S. S. Amritphale,[a] N. Chandra,[a] I.B. Singh[a]

Received (in XXX, XXX) Xth XXXXXXXXX 20XX, Accepted Xth XXXXXXXXX 20XX

DOI: 10.1039/b000000x

Prompted by recent research studies on the higher catalytic efficiency of the Mn_2O_3 over MnO_2, efforts have been made to develop nanostructured MnO_2 and Mn_2O_3, and explore their comparative electrocatalytic response for water oxidation.

Water oxidation reaction has always been seen as a key reaction for the production of hydrogen; an alternative energy source of future fuels.[1-3] In a water splitting process, the anodic reaction that involves four electrons transfer is energetically more demanding and often requires the catalyst to accomplish the oxygen production at a relatively lower overpotential.[4-6] The challenge in this process is the development of an efficient catalyst made of cost effective, non toxic elements. So far, the maximum efficiency has been achieved by using metal oxides or complexes based on metal ions such as Ru and Ir.[7-10] However, the limited availability and higher price of metals such as Ru and Ir, limit their use from large scale application. Nature is able to accomplish the water oxidation reaction efficiently using visible light and a molecular system (oxygen evolution center, OEC) consisting of a cheap and abundant element manganese. The OEC cluster has been reported to have structure Mn_4O_xCa cluster.[11] It is believed that the higher efficiency of the system lies in the ability of the Mn metal ion to switch between different redox states in presence of visible light.

Inspired by nature, many manganese complexes and oxides have been synthesized and demonstrated as water oxidation catalyst.[3,6,12-16] Manganese oxides have been reported to be present in different polymorphs with different crystal structures as well as in different oxidation states of Mn. The impact of the crystal structure of the manganese oxides on the water oxidation catalytic activity has not yet been systematically explored. Rao et al. has synthesized Mn_2O_3 using sol-gel method and demonstrated that the material is an efficient water oxidation catalyst with turnover frequency of 5 x 10^{-4} s^{-1}.[17] Frei et al. also reported efficient water oxidation catalyst by different phases of manganese oxide impregnated in silica nanoparticles and concluded that among different phases, Mn_2O_3 showed the best response for water oxidation activity.[18] It has been proposed that the presence of Mn in +3 oxidation states in manganese tri oxide (Mn_2O_3) provides a favourable electronic environment that makes it an excellent catalyst among other oxides. Recently, Jiao et al. have shown that the crystal structure and the morphology of MnO_2 have no impact on the photocatalytic response towards water oxidation.[19] They demonstrated that the activity is strongly dependent on the surface area of the materials. In all the specified studies, the water oxidation catalysis has been achieved using $[Ru(bpy)_3]^{2+}$ as a photosensitizer and persulfate as a sacrificial agent. The catalysis driven by chemicals has its own benefits but is not favourable for the practical applications. However, the electrochemical water oxidation catalysis offers a way to fabricate the electrodes that can be used for large scale production of hydrogen.

The present work is focussed on further exploration of the morphology *versus* oxidation states of Mn in manganese oxide for water oxidation reaction. We focussed on the synthesis of nanostructured β-MnO_2 and Mn_2O_3 and investigated their electrochemical catalytic response for water oxidation. To the best of our knowledge, Mn_2O_3 nanorods have never been implemented as an electrochemical water oxidation catalyst in literature. We hereby demonstrate that the oxidation state of Mn in manganese oxide has strong impact on the electrocatalytic response towards water oxidation reaction.

First, the synthesis of β-MnO_2 was carried out under hydrothermal conditions following a literature procedure.[20] The synthesis process has been briefly mentioned in the supporting information. The synthesized β-MnO_2 was then acid treated by immersing β-MnO_2 in a solution of 1 M HNO_3 for overnight. In a next step, the acid untreated β-MnO_2 was calcined at 600°C for one hour to get the Mn_2O_3. β-MnO_2, acid treated β-MnO_2 and Mn_2O_3 will be abbreviated as L-MnO_2, L1-MnO_2 and L-Mn_2O_3 respectively in further discussion.

The synthesized manganese oxide was first characterized by powder X-ray diffraction method (PXRD) (Fig.1). Well defined XRD patterns obtained for different samples confirmed the high crystalline nature of the synthesised manganese oxide. As can be seen from Fig.1 and is consistent with the literature report that the PXRD pattern of L-MnO_2 matches with the majority of the phases attributed to the β-MnO_2 phase.[21] This PXRD pattern confirms that the synthesized manganese oxide had β-MnO_2 structure. However, there is also minor contribution of other phase that can be indexed to the α-Mn_2O_3 bixbyte phase.[21] The

[a] *Advance Material and Process Research Institute, Bhopal, India E-mail: archanas002@gmail.com*

[b] *Indian Institute of Science Education and Research, Bhopal, India.*

† Electronic Supplementary Information (ESI) available: [details of any supplementary information available should be included here]. See DOI: 10.1039/b000000x/

formation of mixture of two phases during the hydrothermal synthesis of manganese oxide has previously been observed by Kim and group.[21] The synthesized manganese oxide was then subjected to acid treatment. Interestingly, as can be seen from Fig.1 that the corresponding PXRD of the acid treated sample shows the complete disappearance of the contribution from the α-Mn_2O_3 and the peaks corresponding to only β-MnO_2 phase remains. Dismukes et al. demonstrated a significant increase in the catalytic efficiency on acid treatment of $LiMn_2O_4$.[22] The increase in the catalytic response was attributed to the delithiation of $LiMn_2O_4$ and formation of λ-MnO_2 with cubical Mn_4O_4 cores as active sites to carry out water oxidation catalysis. However, on acid treatment, a change in the oxidation state of Mn was observed. Nitric acid is a well known oxidant and it may be possible that due to the acid treatment, the amount of Mn present in the +3 state as Mn_2O_3 undergo oxidation to produce completely pure β-MnO_2 phase. It is a known fact that on calcination at temperature higher than 500°C MnO_2 results in the formation of manganese oxide with Mn in lower oxidation state than +4. Calcination at 600°C produces α-Mn_2O_3 phase, which is considered as the most interesting phase from the catalytic point of view. Samples were further annealed at 600°C for an hour.[18] Corresponding PXRD of L-Mn_2O_3 clearly confirms the formation of pure α-Mn_2O_3 phase with no remaining contribution from the MnO_2.

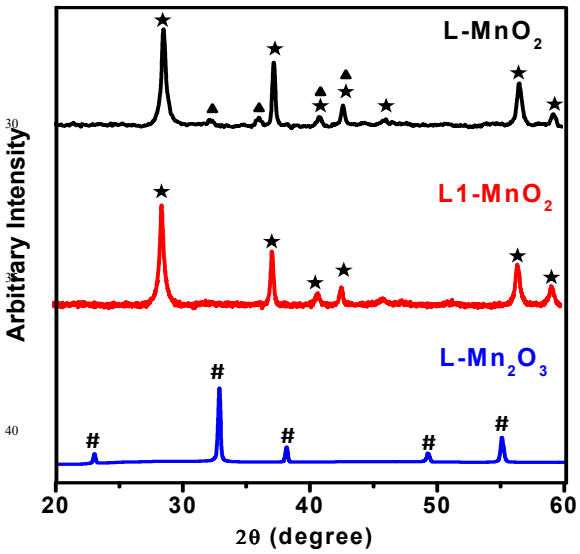

Fig. 1: Top; PXRD patterns obtained for L-MnO_2, L1-MnO_2 and L-Mn_2O_3.where ★ refers to the peaks corresponding to the β-MnO_2 phase, Δ refers to the contribution of Mn_2O_3 in the β-MnO_2 and # refers to the peak corresponding to pure Mn_2O_3 phase.

The results obtained from XRD were further complemented with the XPS measurements (Fig. S1). The oxidation state of Mn was determined by the position of the Mn 2p multiplet splitting for both the samples. According to literature reported by various groups, for different manganese oxides, the peak between 641.8 to 646.8 eV has been assigned for Mn(IV) while for Mn(III) corresponding peak is observed between 641.3 to 641.9 eV.[23-26] $2p_{3/2}$ position for the MnO_2 sample was obtained at 641.8 eV, while for Mn_2O_3 the peak shifts to the lower energy side at 641.6 eV. The shift in the peak position from higher (for L-MnO_2) to lower energy (for L-Mn_2O_3) clearly suggests that annealing of the MnO_2 results in the reduction of valence state of Mn. The Mn 2p spectra were further deconvlouted to determine the presence of variable Mn valence states. However, it was realised that deconvolution of the L-MnO_2 spectra revealed no multiplet splitting pattern, suggesting the absence of the significant contribution of Mn in different valence states. However, deconvoluted L-Mn_2O_3 spectra consist of the multiplets as has been reported by other groups (Fig. 1).[24,25] Position of different multiplets along with their percentage contribution has been summarized in Table S1. The deconvolution indicates the maximum contribution from the peak at 641.3, that has been attributed to the Mn(III) in Mn_2O_3 in literature,[26] indicating the presence of Mn in +3 state in L-Mn_2O_3. Although the results show the decrease in the binding energy for L-Mn2O3 compared to L1-MnO2 still the position of 2p3/2 for two samples are too close making it bit difficult to justify the change in oxidation state.

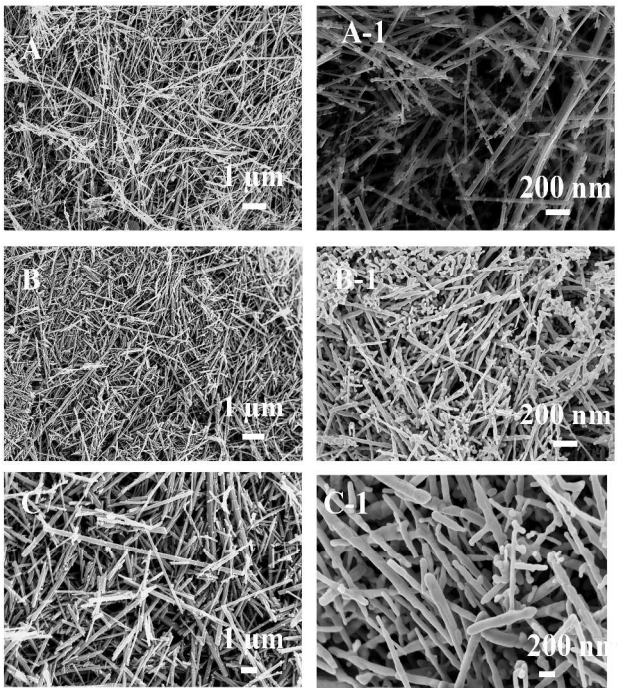

Fig. 2: Low (left hand side) and high (right hand side) magnification SEM images of the L-MnO_2 (A, A-1), L1-MnO_2 (B, B-1) and L-Mn_2O_3 (C, C-1).

To further support the presence of Mn in +3 oxidation in L-Mn_2O_3, oxides were further characterized by the electrochemical method. As has been reported by Nathan et al that CV of Mn_2O_3 film in alkaline medium shows the anodic and cathodic peak corresponding to the oxidation followed by reduction of Mn in Mn_2O_3 however MnO_2 did not show any such pattern under similar experimental conditions.[27] The CV recorded (Fig. S1) for the L-Mn_2O_3 showed oxidation peak at 0.140 V *vs* Ag/AgCl and reduction peak at 0.07 V vs Ag/AgCl in 1 M NaOH electrolyte. However, we did not find any such feature for L-MnO_2 film. Although the trend is same as reported by Nathan but there is difference in the obtained redox potential value. We

assume that the difference is due to the different choice of the substrates.In present case ITO was used as substrate while Nathan et al have used stainless steel. These results also supports that the Mn in L- Mn_2O_3 is present in lower oxidation state compared to L-MnO_2.

Morphology of the L-MnO_2, L1-MnO_2 and L-Mn_2O_3 was further analysed by scanning electron microscopic (SEM) experiments (Fig. 2). The morphology of L-MnO_2 shows that it was consist of nanowires of the length ranging from 2.5–1 µm. The thicknesses of the wires were in between 10-20 nm. On acid treatment, the morphology remains unchanged and nanowires with the length ranging between 3–0.5 µm were observed. The thicknesses of the nanowires were found to be between 10-25 nm. The images of both L-MnO_2 and L1-MnO_2 also showed that some structure grown along with the nanowires. We assume that these are the structure that is not grown completely to the nanowire morphology during the synthesis. On calcination, the morphology of the L-Mn_2O_3 changed little bit with wider diameter between 150–200 nm and length of 4–1 µm.

Electrochemical water oxidation catalysis was performed using a three electrode electrochemical cell. Manganese oxide coated on ITO conducting glass, Ag/AgCl (3 M KCl), and Pt sheet were used as working electrode, reference electrode and counter electrode respectively. Linear scan voltammograms (LSV) were recorded for different films in 1 M NaOH and shown in Fig. 3. L-MnO_2 film showed the water oxidation catalytic activity at the onset potential of 0.970 V (overpotential of ~ 0.570 V) while the overpotential further increased for the L1-MnO_2 film with the onset potential of 1.115 V (overpotential of 0.715 V, inset of Fig. 3). On the other hand for L-Mn_2O_3 this onset potential shifted significantly to a negative potential at 0.685 V corresponding to the overpotential of only 0.285 V. Not only an impressive over-potential drop was observed but also significant current density was obtained at relatively low overpotential for the L-Mn_2O_3 film. Current density of 1 mA/cm^2 was observed for the L-Mn_2O_3 films at an overpotential of just 0.40 V.

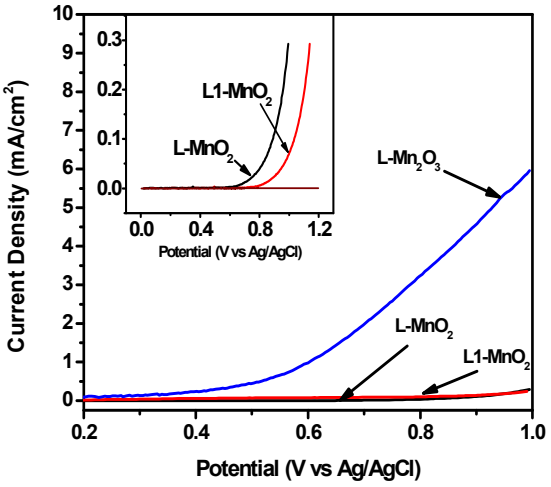

Fig. 3: Linear scan voltammograms for L-MnO_2, L1-MnO_2 and L-Mn_2O_3 films recorded in 1 M NaOH at scan rate of 5 mV/sec. Inset shows the magnified image of the LSV of the L-MnO_2 film and L1-MnO_2 film with difference in the onset potential of water oxidation activity. Inset also shows the LSV of Mn_2O_3 film recorded in 0.1 M $TBAPF_6$/acetonitrile solvent (brown color trace).

To further prove that the observed current is due to the water oxidation, LSV of the L-Mn_2O_3 film was recorded in acetonitrile solvent (0.1 M tetrabutyl ammonium hexafluro phosphate electrolyte solution, inset of Fig. 3). The figure shows that no current was observed in the absence of water. LSV of the films coated with the binder and charcoal only also did not show any significant activity in the 1 M NaOH electrolyte under same experimental conditions. Also, LSV of the L-Mn_2O_3 films were recorded in different volumes percentage of water to organic solvent (acetonitrile). As can be seen from Fig. S2, that as the percentage volume of water to the acetonitrile increases the observed current also increases monotonically thus confirming that water is source for the obtained current. These observations are strong evidence suggesting that the current observed arises primarily from water oxidation and both manganese oxide and water are necessary for the observed current density. However, logical step would be to determine the Faradic efficiency by quantifying the oxygen and hydrogen production. Assuming all the Mn present in the L-Mn_2O_3 film are catalytically active, the turnover frequency was found to be $1x10^{-3}$ s^{-1} at 0.400 V overpotential which is higher by a factor of 10 than observed in recent work where $5x10^{-4}$ s^{-1} turnover frequency was observed at overpotential of ~ 0.38 V in presence of 100 W halogen lamp with the light intensity kept equivalent to 25,000 flux.[17] However, based on the available information in the literature on the catalytic activity of the Mn_2O_3, proper comparison cannot be made since in all the previous studies the driving forces were chemical oxidant as well as the light. In order to check the photoresponse of the film, LSV of films were recorded in NaOH in presence of bias and light (Fig. S3). A small increase in current was observed for L-Mn_2O_3 at higher potentials; however for L-MnO_2 no increase in the activity was obtained. Further efforts will be made in future like doping with different metal ions in an effort to enhance the photo response of these catalysts.

To further explore the reason for the observed difference in the catalytic activity, surface area measurements were performed using Brunauer-Emmett-Teller (BET) method. L-MnO_2, L1-MnO_2 and L-Mn_2O_3 samples were found to have surface areas of 26, 30 and 5 m^2/g respectively. L-MnO_2 and L1-MnO_2 have nearly same surface area which is also consistent with the SEM images of both oxides as they did not show any change at all in the morphology before and after acid treatment. The surface area of the L-Mn_2O_3 films was found to be significantly less than the L-MnO_2 and L1-MnO_2. The decrease in surface area of L-Mn_2O_3 may be due to the transformation of the morphology from nanowires to more like nanorods. These results clearly indicate that the observed difference in activity is due to variation in the oxidation state of Mn.

To further analyse the impact of nanorod like morphology of Mn_2O_3 on the electrochemical water oxidation response, Mn_2O_3 nanoparticles were tested as water oxidation catalyst under similar experimental conditions. Commercial MnO_2 (C-MnO_2) nanoparticles were annealed at 600^{o}C for an hour in order to get the Mn_2O_3 nanoparticles (C-Mn_2O_3).The crystal structure and the morphology of the C-MnO_2 and C-Mn_2O_3 was confirmed using

XRD and SEM (Fig S4 and Fig. S5). The LSV recorded for C-MnO_2 and C- Mn_2O_3 (Fig. S6) clearly demonstrates the higher activity of L-Mn_2O_3 over the C-Mn_2O_3 confirming the importance of nanorod like structure to get higher efficiency. The low activity of the C-Mn_2O_3 may be due to their denser loading compared to the nanorod structure. As has been observed by Dyer[28] that for NiO_x denser loading results in the blockage effect. Because of morphology of the C-Mn_2O_3, it may result in limited exposure to the electrolyte which may not allow the participation of the all the Mn center in the water oxidation reaction, on contrary morphology of Nano rod like structure may lead to the higher participation of the metal center relative to the naanoparticles and thus result in the higher efficiency. Also the C-Mn_2O_3 outperforms the C-MnO_2 and L1-MnO_2 again suggesting that oxide with Mn in +3 state is highly favorable to achieve higher electrochemical catalytic response over +4 state.

Among different samples L-MnO_2, L1-MnO_2 and L-Mn_2O_3 as water oxidation catalyst, it was observed that although all of the manganese oxides have very close surface area as suggested by the surface area measurements value, they significantly differ in their electrocatalytic response. Presence of the manganese ion in +3 oxidation state has been demonstrated as an important factor for the design of the electrocatalyst with improved catalytic response, [17, 29, 30] however there is no clear understanding for the role of the presence of Mn in +3 state to achieve efficient catalysis. Recent work done by Rao et al suggests that trivalency of Mn ions provide appropriate electronic environment around the metal ion of the electrocatalyst that increases its accessibility towards the oxygen and related intermediates species during the electrochemical oxygen evolution process and thereby results in better performance.[17] It was proposed that the presence of $1e^-$ in the antibonding orbital for Mn^{3+} ion (t_{2g}^3, e_g^1) results in a strong interaction between the metal center and oxygen that leads to a high catalytic activity of the Mn_2O_3 over MnO_2.[17] It is because of this reason; a significant difference in the onset potential for water oxidation was also observed for L-MnO_2 and L1-MnO_2 (inset of Fig. 3). The later has got some contribution from Mn^{+3} ion due to the presence of Mn_2O_3 while after acid treatment all Mn was oxidized to +4 oxidation state results in higher overpotential required to achieve the water oxidation process.

In summary, we report that the Mn_2O_3 nanorods act as an efficient water oxidation electrocatalyst. The favourable oxidation state of Mn along with its nanorod like structure makes it an efficient electrochemical water oxidation catalyst at fairly low overpotential. The next step forward will be to synthesize Mn_2O_3 nanostructure with different morphology and develop a protocol where solar driven water oxidation catalysis could be achieved.

Acknowledgement: A.S acknowledges the Department of Science and Technology (DST), India for providing the INSPIRE faculty award (Grant no.: IFA-13 CH-112). D.R.C. acknowledges IISER Bhopal for providing a fellowship. We sincerely thank Dr Amit Paul for critically reviewing the manuscript and his feedback.

(1) T. R. Cook, D. K. Dogutan, S. Y. Reece, Y. Surendranath, T.S. Teets and D. G. Nocera *Chem. Rev.,* 2010, **110**, 6474-6502.

(2) J. K. Hurst, *Science,* 2010, **328**, 315-316.

(3) A. Singh and L. Spiccia *Coord. Chem. Rev.,* 2013, **257**, 2607-2623.

(4) H. L. Dau, C. Limberg, T. Reier, M. Risch, S. Roggan and P. Strasser, *ChemCatChem* 2010, **2**, 724-730.

(5) R. Hocking, R. Brimblecombe, L. Y. Chang, A. Singh, M. Cheah, C. Glover, W. Casey and L. Spiccia, *Nature Chem.,* 2011, **3**, 461-467.

(6) A. Singh, R. K. Hocking, S. Chang, B. George, M. Fehr, K. Lips, A. Schnegg and L. Spiccia, *Chem. Mat.,* 2013, **25**, 1098-1108.

(7) S.W. Gersten, G.J. Samuels and T.J. Meyer, *J. Am. Chem. Soc*. 1982, **104**, 4029-4030.

(8) J. Kiwi and M. Graetzel, *Angew. Chem. Int. Ed. Eng,*. 1979, **18**, 624-628.

(9) F. M. Toma, A. Sartorel, M. Lurlo, M. Carraro, P. Parisse, C. Maccato, S. Rapino, B. R. Gonzalez, H. Amenitisch, T. Da Ros, L. Casalis, A. Goldoni, M. Marcaccio, G. Scorrano, G. Scoles, F. Paolucci, M. Prato and M. Bonchio *Nat. Chem.* 2010, **2**, 826-832.

(10) U. Hintermair, S. M. Hashmi, M. Elimelech and R. H. Crabtree, *J. Am. Chem. Soc.,* 2012, **134**, 9785-9795.

(11) Y. Umena, K. Kawakami, J. Shen and N. Kamiya, *Nature* 2011, **473**, 55-61.

(12) M. Yagi and K. Narita, *J. Am. Chem. Soc.* 2004, **126**, 8084.

(13) Y. Gao, T. Åkermark, J. Liu, L. Sun and B. Åkermark, *J. Am. Chem. Soc.* 2009, **131**, 8726-8727.

(14) M. M. Najafpour and V. McKee, *Catal. Commun.,* 2010, **11**, 1032-1034.

(15) B.S. Yao and A.T. Bell, *J. Phys. Chem. C,* 2012, **116**, 8394-8400.

(16) F. Zhou, A. Izgordin, R.K. Hocking, L. Spiccia and D.R. MacFarlane, *Adv. Energy Mater.,* 2012, **2**, 1013-1021.

(17) 600U. Maitra, B. S. Naidu, A. Govindaraj and C. N. R. Rao, *Proc. Natl. Acad. Sci.,* 2013, 110, 11704-11707..

(18) F. Jiao and H. Frei, *Chem. Commun.,* 2010, **46**, 2920-2924.

(19) V. B. Ram Boppana and F. Jiao, *Chem. Commun.,* 2011, **47**, 8973-8976.

(20) X. Wang and Y. Li, *J. Am. Chem. Soc.,* 2002, **124**, 2880-2885

(21) H. J. Kim, J. B. Lee, Y. Kim, M. Jung, J. P. Umek and J. Dolins, *Nanoscale Res. Lett.,* 2007, **2**, 81-86.

(22) D. M. Robinson, Y. B. Go, M. Greenblatt and G. C. Dismukes, *J. Am. Chem. Soc.,* 2010, **132**, 11467-11469.

(23) H. W. Nesbitt and D. Banerjee, *Am. Minerl*., 1998, **83**, 305-315.

(24) R. P. Gupta and S. K. Sen, *Phys. Rev. B.*, 1974, **10**, 71-79.

(25) M. C. Biesinger, B. P. Payne, A. P. Grosvenor, L.N.M. Lau, A. R. Gerson and R. C. Smart, *Appl. Surf. Sci.*, 2011, **257**, 2717-2730.

(26) A. Ramírez, P. Hillebrand, D. Stellmach, M. M. May, P. Bogdanoff and S. Fiechter, *J. Phys. Chem. C.*, 2014, **118**, 14073-14081.

(27) T. Nathan, M. Cloke and A. Prabaharan, *J. Nanomater*. 2008, 1-8.

(28) C.K. Dyer, *J. Electrochem. Soc.,* 1985, **132**, 64-67.

(29) I. Zaharieva, P. Chernev, M. Risch, K. Klinagan, M. Kohlhoff, A. Fisher and H. Dau *Energy Environ. Sci.* 2012, **5**, 7081-7089.

(30) T. Takashima, K. Hashimoto and R. Nakamura, *J. Am. Chem. Soc.,* 2012, **134**, 1519-1527.

Efficient electrochemical water oxidation catalysis by nanostructured Mn_2O_3

A. Singh,*[a] D. Roy Chowdhury,[b] S. S. Amritphale,[a] N. Chandra,[a] I.B. Singh[a]

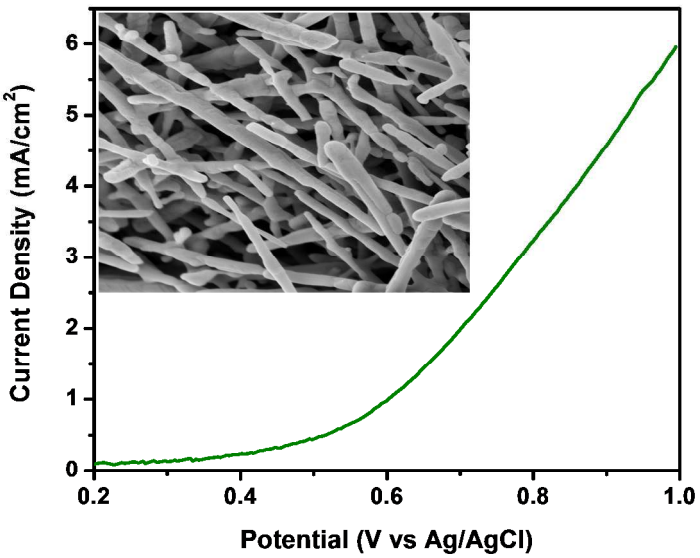

Hydrothermally synthesized Mn_2O_3 nanorods have been demonstrated as efficient electrochemical water oxidation catalyst over the MnO_2 beside the fact that later has high surface area.